Institut für Kommunikations-Technik

Leibniz Universität Hannover

Algebraic Inequalities for MIMO-UWB with Antenna Element Time Delays: Uncorrelated Fading

Bamrung Tau Sieskul, Claus Kupferschmidt, and Thomas Kaiser

in *Proc. IEEE International Conference on Ultra-Wideband 2009 (ICUWB 2009)*, Vancouver, Canada, September 9-11, 2009, pp. 798-803.

This work was supported in part by the integrated European Project, EUWB, under the Contract No. FP7-ICT-215669. The material of this paper was presented in part in EUWB_D3.1.3_v1.0 "Applicationspecific channel modelling with spatial and temporal correlation analysis of the theoretical limits of MIMO-UWB," coExisting short range radio by advanced Ultra-WideBand radio technology (EUWB), Tech. Rep. Deliverable D3.1.3, Jan. 2009.

Algebraic Inequalities for MIMO-UWB with Antenna Element Time Delays: Uncorrelated Fading

Bamrung Tau Sieskul Claus Kupferschmidt Thomas Kaiser
Institute of Communication Technology, Leibniz University Hannover
Appelstraße 9A, 30167 Hanover, Germany, Tel: +49 511 762 2528, Fax: +49 511 762 3030
{bamrung.tausieskul, kupfers, thomas.kaiser}@ikt.uni-hannover.de

***Abstract*—We consider the transmission rate over the multiantenna ultrawideband channel taking into account antenna element time delays. Some algebraic inequalities are explored to formulate the upper bounds on channel capacity. For an uncorrelated fading, the upper bounds can be derived in closed forms. Numerical examples illustrate that in IEEE 802.15.4a channel model, i) the channel capacity tends to be limited when the number of rays increases, and ii) non-line-of-sight channel provides more capacity than line-of-sight channel.**

***Index Terms*—Ultrawideband, multiantenna, channel capacity.**

I. Introduction

As most ultrawideband (UWB) systems operate on several Gigahertz (GHz), an accurate timing characterization is required in order to investigate a real system performance. The accurate timing characterization can be made possible by considering the propagation time along the transceiver. An important feature is the time delay induced by the signal wavefront propagating across antenna elements at each side.

Modeling the channel impulse response to capture spatial characterization, especially angle, is rather diversified. A through framework is the extension of Saleh and Valenzuela's cluster model to the directional channel impulse response (see e.g. [1, eq. (6)] at 7 GHz and [2, eq. (15)] at 2.4 GHz). Recent time delay is modeled including the propagation effect across different antenna elements [3]. However, the channel impulse response in [3] does not take into account the cluster of the rays, which is the attribute of the radio propagation [4].

In this paper, we consider the transmission rate over the multiple-input-multiple-output (MIMO) UWB channel based on the IEEE 802.15.4a channel model including the antenna element time delay (AETD) and an uncorrelated fading. The novelty, merits and contributions can be expressed as follows.

- The novelty of the paper is the approximate determinant upper bound, which appears lower than the well-known Jensen upper bound and also computationally simple for the uncorrelated fading.
- The merits of the paper are the closed forms of the upper bounds on the channel capacity, which is complicate and seems difficult to be found in a closed form.
- The contributions of the paper include the channel statistics of the IEEE 802.15.4a channel model and the evaluation of the channel capacity, by means of its upper bounds, over the standard channel in conjunction with the AETD.

Some algebraic notations are involved as follows. $\log(\cdot)$ denotes the logarithm function of any base. $\mathrm{j}=\sqrt{-1}$ is the unit imaginary number. $\Re(\cdot)$ and $\Im(\cdot)$ are the real and imaginary parts, respectively. $\odot$ is the (element-wise) Hadamard-Schur product. $*$ is the convolution. $\delta(\cdot)$ is the Dirac delta function. $(\cdot)^{\mathrm{T}}$ is the transpose. $(\cdot)^{\mathrm{H}}$ is the Hermitian transpose. $|\cdot|$ is the determinant of a matrix or the absolute value of a scalar. $\mathbf{I}_{(N)}$ denotes the identity matrix of N dimensions. $(\cdot)^{-1}$ is the inverse. $\mathrm{E}_{\mathbf{x}}\{\cdot\}$ is the expectation with respect to $\mathbf{x}$. $\mathbf{A}\preceq\mathbf{B}$ means that $\mathbf{B}-\mathbf{A}$ is positive semi-definite. $\Gamma(x)=\int_0^\infty \mathrm{e}^{-t}t^{x-1}\mathrm{d}t$ is the Euler gamma function. $x\sim\mathcal{N}(\mu_{\mathrm{x}},\sigma_{\mathrm{x}}^2)$ means that x is a Gaussian random variable distributed with mean μ_{x} and the variance σ_{x}^2. $\mathrm{vec}(\cdot)$ is the column-stacking vectorization. $\mathcal{F}\{g(t)\}=\int_{-\infty}^{\infty} g(t)\mathrm{e}^{-\mathrm{j}2\pi ft}\mathrm{d}t$ is the Fouriér transform of $g(t)$. The relation $u(x)=O(v(x))$ means that $u(x)$ is of order less than or equal to $v(x)$.

II. Frequency-Selective MIMO Channel Capacity

Consider a point-to-point communication transceiver consisted of N_{r} receiver and N_{t} transmitter antenna elements, respectively. The received signal $\mathbf{y}(t)\in\mathbb{C}^{N_{\mathrm{r}}\times 1}$ can be expressed as

$$\mathbf{y}(t)=\mathbf{H}(t)*\mathbf{x}(t)+\mathbf{n}(t), \tag{1}$$

where $\mathbf{x}(t)\in\mathbb{C}^{N_{\mathrm{t}}\times 1}$ is the transmitted signal, $\mathbf{H}(t)\in\mathbb{C}^{N_{\mathrm{r}}\times N_{\mathrm{t}}}$ is the MIMO channel, and $\mathbf{n}(t)\in\mathbb{C}^{N_{\mathrm{r}}\times 1}$ is the additive noise.

Theorem 1 (frequency-selective multiantenna channel capacity): Given the frequency-selective channel $\mathbf{H}(t)$ with $\tilde{L}$ multipath components assumed to be known at the receiver and unknown at the transmitter, the channel capacity is provided by

$$C=\max_{\mathbf{\Sigma}_{\mathrm{xx}}(f)}\int_{-\frac{1}{2}W}^{\frac{1}{2}W}\log\left(|\mathbf{I}_{(\check{N})}+\mathbf{M}(f)|\right)\mathrm{d}f, \tag{2}$$

where $\mathbf{\Sigma}_{\mathrm{xx}}(f)$ is the power spectral density (PSD) matrix of the transmitted signal, W is the signal bandwidth, $\check{N}=\min(N_{\mathrm{t}},N_{\mathrm{r}})$ is the minimum number of the transmitter and receiver antennas, and $\mathbf{M}(f)\in\mathbb{C}^{\check{N}\times\check{N}}$ is the matrix given by

$$\mathbf{M}(f)=\begin{cases}\mathbf{\Sigma}_{\mathrm{nn}}^{-1}(f)\mathbf{H}_{\tilde{L}}(f)\mathbf{\Sigma}_{\mathrm{xx}}(f)\mathbf{H}_{\tilde{L}}^{\mathrm{H}}(f), & N_{\mathrm{r}}\le N_{\mathrm{t}},\\ \mathbf{\Sigma}_{\mathrm{xx}}(f)\mathbf{H}_{\tilde{L}}^{\mathrm{H}}(f)\mathbf{\Sigma}_{\mathrm{nn}}^{-1}(f)\mathbf{H}_{\tilde{L}}(f), & N_{\mathrm{r}}>N_{\mathrm{t}},\end{cases} \tag{3}$$

with $\mathbf{H}_{\tilde{L}}(f)$ being the Fouriér transform of the channel and $\mathbf{\Sigma}_{\rm nn}(f)$ being the PSD of the stationary Gaussian noise.

Proof: See [5]. ■

A. Ergodic Capacity

Assume that there exist $\tilde{N}$ random parameters, which are collected in $\boldsymbol{\eta}\in\mathbb{R}^{\tilde{N}\times 1}$, residing in $\mathbf{M}(f)$. When each element of $\boldsymbol{\eta}$ is an ergodic process, the ergodic capacity is written as

$$\bar{C}=\frac{1}{\ln(2)}\int_{-\frac{1}{2}W}^{\frac{1}{2}W}\mathrm{E}_{\boldsymbol{\eta}}\left\{\max_{\mathbf{\Sigma}_{\rm xx}(f)}\ln\left(|\mathbf{I}+\mathbf{M}(\boldsymbol{\eta},f)|\right)\right\}\mathrm{d}f. \quad (4)$$

B. Power Constraint

In (4), the maximization is performed under the constraint $\int_{-\frac{1}{2}W}^{\frac{1}{2}W}\mathrm{tr}\left(\mathbf{\Sigma}_{\rm xx}(f)\right)\mathrm{d}f\le P$, where P is a limited power.

C. Power Spectral Density Constraint

For the UWB system, the power constraint should be replaced by the PSD constraint $\mathbf{\Sigma}_{\rm xx}(f)\preceq\mathbf{\Phi}_{\rm xx}$, where $\mathbf{\Phi}_{\rm xx}\in\mathbb{R}^{N_{\rm t}\times N_{\rm t}}$ is the limited PSD matrix of a certain regulation.

III. IEEE 802.15.4a Channel Model

Based on the Saleh-Valenzuela model [4], the impulse response of the IEEE 802.15.4a channel in complex baseband can be expressed as [6]–[8]

$$h(t)=\sum_{l=0}^{L}\sum_{k=0}^{K}a[k,l]\mathrm{e}^{\mathrm{j}\upsilon[k,l]}\delta(t-T[l]-\tau[k,l]), \quad (5)$$

where $L+1$ is the number of clusters, $K+1$ is the number of multipath rays assumed to be equal in each cluster, $a[k,l]$ is the tap weight of the k-th component in the l-th cluster, $\upsilon[k,l]$ is the corresponding phase shift, and $\tau[k,l]$ is the delay of the k-th multipath component relative to the l-th cluster arrival time $T[l]$. Some channel features can be described as follows [8].

- The number of clusters, $L+1$, is a Poisson random variable with the probability mass function

$$p_L(L)=\frac{1}{L!}\bar{L}^L\mathrm{e}^{-\bar{L}}, \quad (6)$$

  where $\bar{L}$ is the mean of L and tabulated in [8].
- The small-scale amplitude $|a[k,l]|$ is a Nakagami random variable with probability density function (pdf)

$$p_{|a[k,l]|}(x)=\frac{1}{\Gamma(m)}2\left(\frac{m}{\Omega}\right)^m x^{2m-1}\mathrm{e}^{-\frac{m}{\Omega}x^2},\ m\ge\frac{1}{2}, \quad (7)$$

  where $m=\frac{\Omega^2}{\mathrm{E}\{|a[k,l]|^4\}-\Omega^2}$ is the m-factor of the Nakagami distribution, $\Omega=\mathrm{E}\left\{|a[k,l]|^2\right\}$ is the mean-square value of the amplitude. The Nakagami m-factor is a log-normal random variable, whose logarithm has a mean μ_m and a standard deviation σ_m, which depend on the delay by $\mu_m(\tau)=\mu_0-k_m\tau$, and $\sigma_m(\tau)=\tilde{\mu}_0-\tilde{k}_m\tau$, with the mean factors μ_0 and k_m, and the standard deviation factors $\tilde{\mu}_0$ and $\tilde{k}_m$. For the first component of each cluster, the Nakagami m-factor is deterministic and independent of the delay, i.e. $m=\tilde{m}_0$. The mean of the amplitude is given by $\mathrm{E}_{|a[k,l]|}\left\{|a[k,l]|\right\}=\frac{1}{\Gamma(m)}\Gamma\left(m+\frac{1}{2}\right)\left(\frac{\Omega}{m}\right)^{\frac{1}{2}}$ [9, eq. (17)]. We model the amplitude $a[k,l]$ as

$$a[k,l]=\iota|a[k,l]|, \quad (8)$$

  where ι is the sign of the amplitude with an equi-probability of positive and negative values, i.e. with the pdf $p_\iota(x)=\frac{1}{2}\delta(x-1)+\frac{1}{2}\delta(x+1)$. The mean of the small-scale fading becomes zero, i.e. $\mathrm{E}_a\left\{a[k,l]\right\}=0$.
- The phase shift $\upsilon[k,l]$ is uniformly distributed in $[0,2\pi)$.
- The inter-cluster arrival times are distributed as

$$p(T[l]|T[l-1])=\Lambda[l]\mathrm{e}^{-\Lambda[l](T[l]-T[l-1])}, \quad (9)$$

  where $\Lambda[l]$ is the cluster arrival rate assumed to be independent of l.
- The arrival time of the zeroth path in each cluster is zero, i.e. $\tau[0,l]=0$. The ray arrival time is a mixture of two Poisson processes with the conditional pdf

$$p(\tau[k,l]|\tau[k-1,l])=\beta\lambda_1\mathrm{e}^{-\lambda_1(\tau[k,l]-\tau[k-1,l])}+(1-\beta)\lambda_2\mathrm{e}^{-\lambda_2(\tau[k,l]-\tau[k-1,l])}, \quad (10)$$

  where β is the mixture probability parameter, λ_1 and λ_2 are the ray arrival rates.
- In [6], the exact expression of the PDP is given by

$$\mathrm{E}\left\{|a[k,l]|^2|\tau[k,l]\right\}=\frac{1}{\gamma[l]\left((1-\beta)\lambda_1+\beta\lambda_2+1\right)}\Omega[l]\mathrm{e}^{-\frac{1}{\gamma[l]}\tau[k,l]},\ \text{LoS}, \quad (11)$$

  and (12) for some NLoS scenarios, where $\Omega[l]$ is the energy of the l-th cluster and $\gamma[l]$ is the intra-cluster decay time constant, χ is the attenuation of the first component, $\gamma_{\rm r}$ determines how fast the PDP increases to its local maximum and γ_1 determines the decay at later times. For any cluster l in the NLoS in [6]–[8], we shall imply (13). The intra-cluster decay time constant follows

$$\gamma[l]=k_\gamma T[l]+\gamma_0, \quad (14)$$

  where k_γ describes the increase of the decay constant with the delay. The integrated energy of the l-th cluster is dependent on $10\log(\Omega[l])=10\log\left(\mathrm{e}^{-\frac{1}{\Gamma}T[l]}\right)+M_{\rm c}$, where $M_{\rm c}\sim\mathcal{N}(0,\sigma_{\rm c}^2)$ with the standard deviation $\sigma_{\rm c}$. For the logarithm of base 10, we can write in linear scale

$$\Omega[l]=\mathrm{e}^{-\frac{1}{\Gamma}T[l]}10^{\frac{1}{10}M_{\rm c}}. \quad (15)$$

IV. Multiantenna Channel Model

A. Antenna Element Propagation Delay

Assume that the antenna configuration at both ends is uniform linear array, where two adjacent antenna elements are separated by the distance d. The emitted wavefront has an angle $\theta\in(-\pi,\pi]$ with respect to the normal direction of the transmitter antenna array, named angle of departure (AoD). The received wavefront comes up with another angle

$$\mathrm{E}\left\{|a[k,1]|^2|\tau[k,1]\right\} = \frac{\gamma[1]+\gamma_{\mathrm{r}}}{\gamma[1]\left(\gamma[1]+\gamma_{\mathrm{r}}(1-\chi)\right)}\left(1-\chi \mathrm{e}^{-\frac{1}{\gamma_{\mathrm{r}}}\tau[k,1]}\right)\Omega[1]\mathrm{e}^{-\frac{1}{\gamma[1]}\tau[k,1]},\ \text{NLoS in office and industrial.} \tag{12}$$

$$\mathrm{E}\left\{|a[k,l]|^2|\tau[k,l]\right\} = \frac{\gamma[l]+\gamma_{\mathrm{r}}}{\gamma[l]\left(\gamma[l]+\gamma_{\mathrm{r}}(1-\chi)\right)}\left(1-\chi \mathrm{e}^{-\frac{1}{\gamma_{\mathrm{r}}}\tau[k,l]}\right)\Omega[l]\mathrm{e}^{-\frac{1}{\gamma_{l}}\tau[k,l]},\ \text{NLoS in office and industrial.} \tag{13}$$

$\phi \in (-\pi, \pi]$ with respect to the normal direction of the receiver antenna array, named angle of arrival (AoA). For the k-th cluster and the l-th path, both the AoD and the AoA induce the propagation delays[1] $\frac{1}{c}(n_{\mathrm{t}}-1)d\sin(\theta[k,l])$ and $\frac{1}{c}(n_{\mathrm{r}}-1)d\sin(\phi[k,l])$ at the n_{t}-th transmitter and the n_{r}-th receiver antennas, respectively, where c is the wave propagation speed.

The impulse response, which captures the time delay across antenna elements at both sides, can be written as

$$h^{k,l}_{n_{\mathrm{r}},n_{\mathrm{t}}}(t) = \delta(t-\psi_{n_{\mathrm{r}},n_{\mathrm{t}}}[k,l]), \tag{16}$$

where the propagation delay $\psi_{n_{\mathrm{r}},n_{\mathrm{t}}}[k,l]$ is given by

$$\psi_{n_{\mathrm{r}},n_{\mathrm{t}}}[k,l] = \frac{1}{c}d\left((n_{\mathrm{t}}-1)\sin(\theta[k,l])+(n_{\mathrm{r}}-1)\sin(\phi[k,l])\right). \tag{17}$$

For $d = 9$ cm and $c = 3\times 10^8$ m/s, the smallest delay of the $(2,1)$-th link is $\psi_{2,1}[k,l] = 0.3\sin(\theta[k,l])$ ns. For any $\theta[k,l] \in (-\pi,\pi]$, the propagation delay lies in $[-0.3, 0.3]$ ns and can have a significant role in the UWB systems. The above time delay is implicitly mentioned in a design of the integrated circuit [10].

B. Effective Channel Model

The effective channel impulse response $h_{n_{\mathrm{r}},n_{\mathrm{t}}}(t) = h(t) * h^{k,l}_{n_{\mathrm{r}},n_{\mathrm{t}}}(t)$ can be shown as

$$h_{n_{\mathrm{r}},n_{\mathrm{t}}}(t) = \sum_{l=0}^{L}\sum_{k=0}^{K}\alpha_{n_{\mathrm{r}},n_{\mathrm{t}}}[k,l]\delta(t-T[l]-\tau[k,l]-\psi_{n_{\mathrm{r}},n_{\mathrm{t}}}[k,l]), \tag{18}$$

where $\alpha_{n_{\mathrm{r}},n_{\mathrm{t}}}[k,l]$ is the antenna-dependent complex amplitude given by $\alpha_{n_{\mathrm{r}},n_{\mathrm{t}}}[k,l] = a_{n_{\mathrm{r}},n_{\mathrm{t}}}[k,l]\mathrm{e}^{\mathrm{j}\upsilon_{n_{\mathrm{r}},n_{\mathrm{t}}}[k,l]}$.

C. Random Parameters

In the system discussed previously, there are $\tilde{N} = 4KLN_{\mathrm{r}}N_{\mathrm{t}} + L(K+1) + 1$ random parameters, i.e. $\boldsymbol{\eta} \in \mathbb{C}^{(4KLN_{\mathrm{r}}N_{\mathrm{t}}+L(K+1)+1)\times 1}$, which can be written as

$$\boldsymbol{\eta} = \begin{bmatrix}\mathbf{a}^{\mathrm{T}} & \boldsymbol{\upsilon}^{\mathrm{T}} & \boldsymbol{\phi}^{\mathrm{T}} & \boldsymbol{\theta}^{\mathrm{T}} & \boldsymbol{\delta}^{\mathrm{T}} & M_{\mathrm{c}}\end{bmatrix}^{\mathrm{T}}, \tag{19}$$

where $\mathbf{a} \in \mathbb{C}^{KLN_{\mathrm{r}}N_{\mathrm{t}}\times 1}$, $\boldsymbol{\upsilon} \in \mathbb{R}^{KLN_{\mathrm{r}}N_{\mathrm{t}}\times 1}$, $\boldsymbol{\phi} \in \mathbb{R}^{KLN_{\mathrm{r}}N_{\mathrm{t}}\times 1}$, $\boldsymbol{\theta} \in \mathbb{R}^{KLN_{\mathrm{r}}N_{\mathrm{t}}\times 1}$, and $\boldsymbol{\delta} \in \mathbb{R}^{L(K+1)\times 1}$ are given by

$$\mathbf{a} = \mathrm{vec}(\mathbf{A}),\ \boldsymbol{\upsilon} = \mathrm{vec}(\boldsymbol{\Upsilon}),\ \boldsymbol{\phi} = \mathrm{vec}(\boldsymbol{\Phi}),\ \boldsymbol{\theta} = \mathrm{vec}(\boldsymbol{\Theta}), \tag{20a}$$

$$\boldsymbol{\delta} = \begin{bmatrix}T[1] & \cdots & T[L] & \tau[1,1] & \cdots \\ \tau[1,L] & \tau[2,1] & \cdots & \tau[K,L]\end{bmatrix}^{\mathrm{T}}, \tag{20b}$$

[1]The relative propagation delay can be negative, since the time reference of the antenna array is at the first element.

with $\mathbf{A} \in \mathbb{C}^{KN_{\mathrm{r}}N_{\mathrm{t}}\times L}$, $\boldsymbol{\Upsilon} \in \mathbb{R}^{KN_{\mathrm{r}}N_{\mathrm{t}}\times L}$, $\boldsymbol{\Phi} \in \mathbb{R}^{KN_{\mathrm{r}}N_{\mathrm{t}}\times L}$ and $\boldsymbol{\Theta} \in \mathbb{R}^{KN_{\mathrm{r}}N_{\mathrm{t}}\times L}$ given by

$$\mathbf{A} = \begin{bmatrix}\mathrm{vec}(\mathbf{A}[1,1]) & \cdots & \mathrm{vec}(\mathbf{A}[1,L]) \\ \vdots & \ddots & \vdots \\ \mathrm{vec}(\mathbf{A}[K,1]) & \cdots & \mathrm{vec}(\mathbf{A}[K,L])\end{bmatrix}, \tag{21a}$$

$$\boldsymbol{\Upsilon} = \begin{bmatrix}\mathrm{vec}(\boldsymbol{\Upsilon}[1,1]) & \cdots & \mathrm{vec}(\boldsymbol{\Upsilon}[1,L]) \\ \vdots & \ddots & \vdots \\ \mathrm{vec}(\boldsymbol{\Upsilon}[K,1]) & \cdots & \mathrm{vec}(\boldsymbol{\Upsilon}[K,L])\end{bmatrix}, \tag{21b}$$

$$\boldsymbol{\Phi} = \begin{bmatrix}\mathrm{vec}(\boldsymbol{\Phi}[1,1]) & \cdots & \mathrm{vec}(\boldsymbol{\Phi}[1,L]) \\ \vdots & \ddots & \vdots \\ \mathrm{vec}(\boldsymbol{\Phi}[K,1]) & \cdots & \mathrm{vec}(\boldsymbol{\Phi}[K,L])\end{bmatrix}, \tag{21c}$$

$$\boldsymbol{\Theta} = \begin{bmatrix}\mathrm{vec}(\boldsymbol{\Theta}[1,1]) & \cdots & \mathrm{vec}(\boldsymbol{\Theta}[1,L]) \\ \vdots & \ddots & \vdots \\ \mathrm{vec}(\boldsymbol{\Theta}[K,1]) & \cdots & \mathrm{vec}(\boldsymbol{\Theta}[K,L])\end{bmatrix}, \tag{21d}$$

with $\mathbf{A}[k,l] \in \mathbb{C}^{N_{\mathrm{r}}\times N_{\mathrm{t}}}$, $\boldsymbol{\Upsilon}[k,l] \in \mathbb{R}^{N_{\mathrm{r}}\times N_{\mathrm{t}}}$, $\boldsymbol{\Phi}[k,l] \in \mathbb{R}^{N_{\mathrm{r}}\times N_{\mathrm{t}}}$ and $\boldsymbol{\Theta}[k,l] \in \mathbb{R}^{N_{\mathrm{r}}\times N_{\mathrm{t}}}$ given by

$$\mathbf{A}[k,l] = \begin{bmatrix}a_{1,1}[k,l] & \cdots & a_{1,N_{\mathrm{t}}}[k,l] \\ \vdots & \ddots & \vdots \\ a_{N_{\mathrm{r}},1}[k,l] & \cdots & a_{N_{\mathrm{r}},N_{\mathrm{t}}}[k,l]\end{bmatrix}, \tag{22a}$$

$$\boldsymbol{\Upsilon}[k,l] = \begin{bmatrix}\upsilon_{1,1}[k,l] & \cdots & \upsilon_{1,N_{\mathrm{t}}}[k,l] \\ \vdots & \ddots & \vdots \\ \upsilon_{N_{\mathrm{r}},1}[k,l] & \cdots & \upsilon_{N_{\mathrm{r}},N_{\mathrm{t}}}[k,l]\end{bmatrix}, \tag{22b}$$

$$\boldsymbol{\Phi}[k,l] = \begin{bmatrix}\phi_{1,1}[k,l] & \cdots & \phi_{1,N_{\mathrm{t}}}[k,l] \\ \vdots & \ddots & \vdots \\ \phi_{N_{\mathrm{r}},1}[k,l] & \cdots & \phi_{N_{\mathrm{r}},N_{\mathrm{t}}}[k,l]\end{bmatrix}, \tag{22c}$$

$$\boldsymbol{\Theta}[k,l] = \begin{bmatrix}\theta_{1,1}[k,l] & \cdots & \theta_{1,N_{\mathrm{t}}}[k,l] \\ \vdots & \ddots & \vdots \\ \theta_{N_{\mathrm{r}},1}[k,l] & \cdots & \theta_{N_{\mathrm{r}},N_{\mathrm{t}}}[k,l]\end{bmatrix}. \tag{22d}$$

V. Uncorrelated Noise and Signal

Assume that the additive noise at the receiver is independent of each other, strict-sense such that the noise covariance is independent of the time lag and has an identical variance σ^2_{n}, and independent of the frequency. Then, the noise covariance becomes $\mathbf{R}_{\mathrm{nn}}(\tau) = \mathrm{E}_{\mathbf{n}(t)}\{\mathbf{n}(t)\mathbf{n}^{\mathrm{H}}(t-\tau)\} = \sigma^2_{\mathrm{n}}\mathbf{I}\delta(\tau)$. Using the Fouriér transform of the impulse function $\mathcal{F}\{\delta(\tau)\} = 1$, the noise power spectrum becomes $\boldsymbol{\Sigma}_{\mathrm{nn}}(f) = \sigma^2_{\mathrm{n}}\mathbf{I}$. Substituting $\boldsymbol{\Sigma}_{\mathrm{nn}}(f) = \sigma^2_{\mathrm{n}}\mathbf{I}$ into (3) and (2), we obtain a similar expression to [11, eq. (79)]. Usually, the transmitted signal that maximizes the mutual information is the uncorrelated

Gaussian signal. If the signal variance is identically σ_{x}^2, we obtain $\mathbf{R}_{\mathrm{xx}}(\tau) = \mathrm{E}_{\mathbf{x}(t)}\{\mathbf{x}(t)\mathbf{x}^{\mathrm{H}}(t-\tau)\} = \sigma_{\mathrm{x}}^2\mathbf{I}\delta(\tau)$. Then, it follows $\mathbf{\Sigma}_{\mathrm{xx}}(f) = \sigma_{\mathrm{x}}^2\mathbf{I}$. We can see that $\mathbf{H}_{\check{L}}(f)$ in Theorem 1 is equivalent to

$$\mathbf{H}_{K,L}(f) = \sum_{l=0}^{L}\sum_{k=0}^{K} \mathrm{e}^{-\mathrm{j}2\pi f(T[l]+\tau[k,l])}\mathbf{B}[k,l], \tag{23}$$

where $\mathbf{B}[k,l] \in \mathbb{C}^{N_{\mathrm{r}}\times N_{\mathrm{t}}}$ is given by $\mathbf{B}[k,l] = \mathbf{A}[k,l] \odot \mathrm{e}^{j\mathbf{\Upsilon}[k,l]}$. Substituting $\mathbf{\Sigma}_{\mathrm{nn}}(f) = \sigma_{\mathrm{n}}^2\mathbf{I}$ and $\mathbf{\Sigma}_{\mathrm{xx}}(f) = \sigma_{\mathrm{x}}^2\mathbf{I}$ into (2), we obtain

$$C = \frac{1}{\ln(2)}\int_{-\frac{1}{2}W}^{\frac{1}{2}W} \ln\left(|\mathbf{I}_{(\check{N})} + \mathbf{M}(\boldsymbol{\eta}, f)|\right)\mathrm{d}f, \tag{24}$$

where $\mathbf{M}(\boldsymbol{\eta}, f) \in \mathbb{C}^{\check{N}\times\check{N}}$ is given by

$$\mathbf{M}(\boldsymbol{\eta}, f) = \begin{cases} \frac{\sigma_{\mathrm{x}}^2}{\sigma_{\mathrm{n}}^2}\mathbf{H}_{K,L}(f)\mathbf{H}_{K,L}^{\mathrm{H}}(f), & N_{\mathrm{r}} \le N_{\mathrm{t}}, \\ \frac{\sigma_{\mathrm{x}}^2}{\sigma_{\mathrm{n}}^2}\mathbf{H}_{K,L}^{\mathrm{H}}(f)\mathbf{H}_{K,L}(f), & N_{\mathrm{r}} > N_{\mathrm{t}}. \end{cases} \tag{25}$$

VI. Inequalities

A. Jensen Upper Bound

The natural logarithm of the determinant of a positive definite matrix is concave (see e.g. [12, pp. 466-467] and [13, Sec. 17.9.1] for a nonnegative definite symmetric matrix). The ergodic capacity can be upper bounded by

$$\bar{C} \le \bar{B}_{\mathrm{Jensen}} = \frac{1}{\ln(2)}\int_{-\frac{1}{2}W}^{\frac{1}{2}W} \ln\left(|\mathbf{I} + \mathrm{E}_{\boldsymbol{\eta}}\left\{\mathbf{M}(\boldsymbol{\eta}, f)\right\}|\right)\mathrm{d}f, \tag{26}$$

where the inequality is derived from the Jensen's inequality of the real-valued concave function $\ln(|\cdot|)$.

B. Determinant Upper Bounds

We explore a simple inequality $\ln(|\mathbf{M}|) \le \mathrm{tr}(\mathbf{M}) - \check{N}$, which is a property of the determinant (see e.g. [14, p. 55]). We can then write

$$\bar{C} \le \bar{B}_{\mathrm{det}} = \frac{1}{\ln(2)}\int_{-\frac{1}{2}W}^{\frac{1}{2}W} \mathrm{tr}\left(\mathrm{E}_{\boldsymbol{\eta}}\left\{\mathbf{M}(\boldsymbol{\eta}, f)\right\}\right)\mathrm{d}f. \tag{27}$$

If the matrix $\mathbf{M}(\boldsymbol{\eta}, f)$ can be expressed as $\mathbf{M}(\boldsymbol{\eta}, f) = \frac{\sigma_{\mathrm{x}}^2}{\sigma_{\mathrm{n}}^2}\breve{\mathbf{M}}(\boldsymbol{\eta}, f)$, where $\frac{\sigma_{\mathrm{x}}^2}{\sigma_{\mathrm{n}}^2}$ is the signal-to-noise ratio (SNR), the determinant $|\mathbf{I} + \frac{\sigma_{\mathrm{x}}^2}{\sigma_{\mathrm{n}}^2}\breve{\mathbf{M}}(\boldsymbol{\eta}, f)|$ can be expanded into $|\mathbf{I} + \frac{\sigma_{\mathrm{x}}^2}{\sigma_{\mathrm{n}}^2}\breve{\mathbf{M}}(\boldsymbol{\eta}, f)| = 1 + \frac{\sigma_{\mathrm{x}}^2}{\sigma_{\mathrm{n}}^2}\mathrm{tr}\left(\breve{\mathbf{M}}(\boldsymbol{\eta}, f)\right) + O\left(\left(\frac{\sigma_{\mathrm{x}}^2}{\sigma_{\mathrm{n}}^2}\right)^2\right)$ [15, p. 312]. It means that there exists a constant c_1 such that $\left||\mathbf{I} + \frac{\sigma_{\mathrm{x}}^2}{\sigma_{\mathrm{n}}^2}\breve{\mathbf{M}}(\boldsymbol{\eta}, f)| - \left(1 + \frac{\sigma_{\mathrm{x}}^2}{\sigma_{\mathrm{n}}^2}\mathrm{tr}\left(\breve{\mathbf{M}}(\boldsymbol{\eta}, f)\right)\right)\right| \le c_1\left(\frac{\sigma_{\mathrm{x}}^2}{\sigma_{\mathrm{n}}^2}\right)^2$. If the asymptotic expansion is approximated, the approximation error will be small when the SNR $\frac{\sigma_{\mathrm{x}}^2}{\sigma_{\mathrm{n}}^2}$ is low. The ergodic capacity in (4) can be approximated by

$$\begin{aligned}\bar{C} \simeq \tilde{C} &= \frac{1}{\ln(2)}\int_{-\frac{1}{2}W}^{\frac{1}{2}W} \mathrm{E}_{\boldsymbol{\eta}}\left\{\ln\left(1 + \mathrm{tr}\left(\mathbf{M}(\boldsymbol{\eta}, f)\right)\right)\right\}\mathrm{d}f \\ &\le \bar{B}_{\mathrm{approdet}} = \frac{1}{\ln(2)}\int_{-\frac{1}{2}W}^{\frac{1}{2}W} \ln\left(1 + \mathrm{E}_{\boldsymbol{\eta}}\left\{\mathrm{tr}\left(\mathbf{M}(\boldsymbol{\eta}, f)\right)\right\}\right)\mathrm{d}f,\end{aligned} \tag{28}$$

where the inequality holds from the concavity of $\ln(\cdot)$.

C. Trace Upper Bounds

In [11, Lem. 2], an inequality has been invoked in the form of $|\mathbf{M}| \le \left(\frac{1}{\check{N}}\mathrm{tr}(\mathbf{M})\right)^{\check{N}}$. The above inequality is a property of the trace (see e.g. [14, p. 43]). Taking the natural logarithm at both sides, the inequality follows $\ln(|\mathbf{M}|) \le \check{N}\left(\ln\left(\mathrm{tr}(\mathbf{M})\right) - \ln(\check{N})\right)$. The result herein generalizes [11] in that we consider the integral over the whole bandwidth W. It can be shown that

$$\begin{aligned}\bar{C} \le \bar{B}_{\mathrm{tr}} &= \frac{1}{\ln(2)}\check{N}\int_{-\frac{1}{2}W}^{\frac{1}{2}W} \mathrm{E}_{\boldsymbol{\eta}}\left\{\ln\left(1 + \frac{1}{\check{N}}\mathrm{tr}\left(\mathbf{M}(\boldsymbol{\eta}, f)\right)\right)\right\}\mathrm{d}f \\ &\le \bar{B}_{\mathrm{tr+Jensen}} = \frac{1}{\ln(2)}\check{N}\int_{-\frac{1}{2}W}^{\frac{1}{2}W} \ln\left(1 + \frac{1}{\check{N}}\mathrm{E}_{\boldsymbol{\eta}}\left\{\mathrm{tr}\left(\mathbf{M}(\boldsymbol{\eta}, f)\right)\right\}\right)\mathrm{d}f,\end{aligned} \tag{29}$$

where the last inequality holds from the Jensen inequality according to the concavity of $\ln(\cdot)$.

VII. Channel Statistics

A. Amplitude Correlation

Before evaluating the correlation of the amplitude, we consider the dispersion matrix of the amplitude matrix $\tilde{\mathbf{A}}[k,l] = \mathbf{A}[k,l] - \mathrm{E}\{\mathbf{A}[k,l]\} \in \mathbb{C}^{N_{\mathrm{r}}\times N_{\mathrm{t}}}$. From the PDPs of the LoS in (11) and NLoS in (13), there is no correlation for the contributions between k and $\acute{k}$ as well as between l and $\acute{l}$. Then, we have

$$\begin{aligned}\mathbf{\Sigma}_{\mathbf{AA}}[k,l,\acute{k},\acute{l}] &= \mathrm{E}\left\{\mathrm{vec}(\tilde{\mathbf{A}}[k,l])\mathrm{vec}^{\mathrm{H}}(\tilde{\mathbf{A}}[\acute{k},\acute{l}])\right\} \\ &= \delta_{k,\acute{k}}\delta_{l,\acute{l}}\mathrm{E}\left\{|a[k,l]|^2|\tau[k,l]\right\}\mathbf{I}_{(N_{\mathrm{r}}N_{\mathrm{t}})}.\end{aligned} \tag{30}$$

Indeed, the expectation of $\mathrm{E}\left\{|a[k,l]|^2|\tau[k,l]\right\}$ should be averaged over $T[l]$, $\tau[k,l]$ and M_{c}. The overall expectation is shown in (31). The uncorrelated spatial correlation results in

$$\mathrm{E}_{\boldsymbol{\eta}}\{\mathbf{M}(\boldsymbol{\eta}, f)\} = \begin{cases} \frac{\sigma_{\mathrm{x}}^2}{\sigma_{\mathrm{n}}^2}N_{\mathrm{t}}\varsigma\mathbf{I}_{(N_{\mathrm{r}})}, & N_{\mathrm{r}} \le N_{\mathrm{t}}, \\ \frac{\sigma_{\mathrm{x}}^2}{\sigma_{\mathrm{n}}^2}N_{\mathrm{r}}\varsigma\mathbf{I}_{(N_{\mathrm{t}})}, & N_{\mathrm{r}} > N_{\mathrm{t}}, \end{cases} \tag{32}$$

where ς is given by

$$\varsigma = \sum_{L=1}^{\infty}\frac{1}{L!}\bar{L}^L\mathrm{e}^{-\bar{L}}\sum_{l=0}^{L}\sum_{k=0}^{K}\mathrm{E}_{\tau,T,M_{\mathrm{c}}}\left\{|a[k,l]|^2|\tau[k,l]\right\}. \tag{33}$$

It can be proved that ς in (33) is finite. The determinant in (26) and the trace in (27), (28) and (29) can be expressed as

$$|\mathbf{I} + \mathrm{E}_{\boldsymbol{\eta}}\{\mathbf{M}(\boldsymbol{\eta}, f)\}| = \begin{cases} \left(1 + \frac{\sigma_{\mathrm{x}}^2}{\sigma_{\mathrm{n}}^2}N_{\mathrm{t}}\varsigma\right)^{N_{\mathrm{r}}}, & N_{\mathrm{r}} \le N_{\mathrm{t}}, \\ \left(1 + \frac{\sigma_{\mathrm{x}}^2}{\sigma_{\mathrm{n}}^2}N_{\mathrm{r}}\varsigma\right)^{N_{\mathrm{t}}}, & N_{\mathrm{r}} > N_{\mathrm{t}}, \end{cases} \tag{34}$$

$$\mathrm{tr}(\mathrm{E}_{\boldsymbol{\eta}}\{\mathbf{M}(\boldsymbol{\eta}, f)\}) = \frac{\sigma_{\mathrm{x}}^2}{\sigma_{\mathrm{n}}^2}N_{\mathrm{r}}N_{\mathrm{t}}\varsigma. \tag{35}$$

$$\mathrm{E}_{\tau,T,M_\mathrm{c}}\left\{|a[k,l]|^2|\tau[k,l]\right\}$$
$$=\begin{cases}\frac{1}{(1-\beta)\lambda_1+\beta\lambda_2+1}\mathrm{E}\left\{\frac{1}{\gamma[l]}\mathrm{e}^{-\frac{1}{\Gamma}T[l]}\right\}\mathrm{E}\left\{\mathrm{e}^{-\frac{1}{\gamma[l]}\tau[k,l]}\right\}\mathrm{E}\left\{10^{\frac{1}{10}M_\mathrm{c}}\right\}, & \text{LoS},\\ \mathrm{E}\left\{\frac{\gamma[l]+\gamma_\mathrm{r}}{\gamma[l](\gamma[l]+\gamma_\mathrm{r}(1-\chi))}\mathrm{e}^{-\frac{1}{\Gamma}T[l]}\right\}\left(\mathrm{E}\left\{\mathrm{e}^{-\frac{1}{\gamma[l]}\tau[k,l]}\right\}-\chi\mathrm{E}\left\{\mathrm{e}^{-\left(\frac{1}{\gamma_\mathrm{r}}+\frac{1}{\gamma[l]}\right)\tau[k,l]}\right\}\right)\mathrm{E}\left\{10^{\frac{1}{10}M_\mathrm{c}}\right\}, & \text{NLoS in office and industrial.}\end{cases} \tag{31}$$

B. PDP Expectation

For $\gamma[l]=k_\gamma T[l]+\gamma_0$ in (14), the channel models CM1 - CM7 and CM9 (outdoor LoS, outdoor NLoS, and farm environments) provide $k_\gamma=0$ or the non-assigned value of k_γ, while the channel models CM8 and CM9 (industrial) have $k_\gamma=0.926$ for LoS and the non-assigned value of k_γ for NLoS. For the case in which $\gamma[l]$ is independent of $T[l]$, i.e. $k_\gamma=0$, the expectation involving $\gamma[l]$ remains a simple expression, while the case of $\gamma[l]$ dependent on $T[l]$ causes a complicate integration. For the NLoS scenario, there is no requirement to calculate the statistical mean of $\mathrm{E}\left\{|a[k,l]|^2|\tau[k,l]\right\}$ depending on k_γ, since there is no tabulated data of k_γ.

1) LoS Expectation: Under the LoS condition, we have

$$\mathrm{E}\left\{\frac{1}{\gamma[l]}\mathrm{e}^{-\frac{1}{\Gamma}T[l]}\right\}=\frac{1}{\gamma[l]\left(\Gamma\Lambda+1\right)^l}\Gamma^l\Lambda^l, \tag{36}$$

and for non-zero k_γ,

$$\mathrm{E}\left\{\frac{1}{\gamma[l]}\mathrm{e}^{-\frac{1}{\Gamma}T[l]}\right\}=\frac{1}{(l-1)!}\Lambda^l\int_0^\infty\frac{1}{k_\gamma x+\gamma_0}x^{l-1}\mathrm{e}^{-\left(\frac{1}{\Gamma}+\Lambda\right)x}\mathrm{d}x. \tag{37}$$

The characteristic function of two Poisson processes results in

$$\mathrm{E}\left\{\mathrm{e}^{-\frac{1}{\gamma[l]}\tau[k,l]}\right\}=\left(\frac{\lambda_1\gamma[l]}{\lambda_1\gamma[l]+1}\right)^k\beta+\left(\frac{\lambda_2\gamma[l]}{\lambda_2\gamma[l]+1}\right)^k(1-\beta), \tag{38}$$

and for non-zero k_γ,

$$\mathrm{E}\left\{\mathrm{e}^{-\frac{1}{\gamma[l]}\tau[k,l]}\right\}=\frac{1}{(l-1)!}\Lambda^l\int_0^\infty\left(\left(\frac{\lambda_1(k_\gamma x+\gamma_0)}{\lambda_1(k_\gamma x+\gamma_0)+1}\right)^k\beta+\left(\frac{\lambda_2(k_\gamma x+\gamma_0)}{\lambda_2(k_\gamma x+\gamma_0)+1}\right)^k(1-\beta)\right)x^{l-1}\mathrm{e}^{-\Lambda x}\mathrm{d}x. \tag{39}$$

Using $\int_{-\infty}^{\infty}\mathrm{e}^{-p^2x^2\pm qx}\mathrm{d}x=\frac{1}{p}\sqrt{\pi}\mathrm{e}^{\frac{1}{4p^2}q^2}$ (see e.g. [16, p. 337] and [17, p. 65]), the shadowing effect can be written as

$$\mathrm{E}_{M_\mathrm{c}}\left\{10^{\frac{1}{10}M_\mathrm{c}}\right\}=\mathrm{e}^{\frac{1}{200}\ln^2(10)\sigma_\mathrm{c}^2}. \tag{40}$$

2) NLoS Expectation: One of the expectation for the NLoS $\mathrm{E}\left\{\frac{\gamma[l]+\gamma_\mathrm{r}}{\gamma[l](\gamma[l]+\gamma_\mathrm{r}(1-\chi))}\mathrm{e}^{-\frac{1}{\Gamma}T[l]}\right\}$ can be expressed as

$$\mathrm{E}\left\{\frac{\gamma[l]+\gamma_\mathrm{r}}{\gamma[l]\left(\gamma[l]+\gamma_\mathrm{r}(1-\chi)\right)}\mathrm{e}^{-\frac{1}{\Gamma}T[l]}\right\}=\frac{\gamma[l]+\gamma_\mathrm{r}}{\gamma[l]\left(\gamma[l]+\gamma_\mathrm{r}(1-\chi)\right)\left(\Gamma\Lambda+1\right)^l}\Gamma^l\Lambda^l. \tag{41}$$

Modified from (38), the expectation $\mathrm{E}\left\{\mathrm{e}^{-\left(\frac{1}{\gamma_\mathrm{r}}+\frac{1}{\gamma[l]}\right)\tau[k,l]}\right\}$ can be explicitly written as

$$\mathrm{E}\left\{\mathrm{e}^{-\left(\frac{1}{\gamma_\mathrm{r}}+\frac{1}{\gamma[l]}\right)\tau[k,l]}\right\}=\left(\frac{\lambda_1\gamma_\mathrm{r}\gamma[l]}{\lambda_1\gamma_\mathrm{r}\gamma[l]+\gamma_\mathrm{r}+\gamma[l]}\right)^k\beta+\left(\frac{\lambda_2\gamma_\mathrm{r}\gamma[l]}{\lambda_2\gamma_\mathrm{r}\gamma[l]+\gamma_\mathrm{r}+\gamma[l]}\right)^k(1-\beta). \tag{42}$$

VIII. Upper Bounds

From (26) and (34), we have the Jensen bound in closed form

$$\bar{B}_\mathrm{Jensen}=\begin{cases}\frac{1}{\ln(2)}WN_\mathrm{r}\ln\left(1+\frac{\sigma_\mathrm{x}^2}{\sigma_\mathrm{n}^2}N_\mathrm{t}\varsigma\right), & N_\mathrm{r}\le N_\mathrm{t},\\ \frac{1}{\ln(2)}WN_\mathrm{t}\ln\left(1+\frac{\sigma_\mathrm{x}^2}{\sigma_\mathrm{n}^2}N_\mathrm{r}\varsigma\right), & N_\mathrm{r}>N_\mathrm{t}.\end{cases} \tag{43}$$

From (27) and (35), the determinant upper bound yields

$$\bar{B}_\mathrm{det}=\frac{1}{\ln(2)}\frac{\sigma_\mathrm{x}^2}{\sigma_\mathrm{n}^2}WN_\mathrm{r}N_\mathrm{t}\varsigma. \tag{44}$$

From (28) and (35), the determinant capacity using low $\frac{\sigma_\mathrm{x}^2}{\sigma_\mathrm{n}^2}$ approximation is given by

$$\bar{B}_\mathrm{approdet}=\frac{1}{\ln(2)}W\ln\left(1+\frac{\sigma_\mathrm{x}^2}{\sigma_\mathrm{n}^2}N_\mathrm{r}N_\mathrm{t}\varsigma\right). \tag{45}$$

From (29) and (35), the upper bound based on trace and Jensen inequality can be written as

$$\bar{B}_\mathrm{tr+Jensen}=\begin{cases}\frac{1}{\ln(2)}WN_\mathrm{r}\ln\left(1+\frac{\sigma_\mathrm{x}^2}{\sigma_\mathrm{n}^2}N_\mathrm{t}\varsigma\right), & N_\mathrm{r}\le N_\mathrm{t},\\ \frac{1}{\ln(2)}WN_\mathrm{t}\ln\left(1+\frac{\sigma_\mathrm{x}^2}{\sigma_\mathrm{n}^2}N_\mathrm{r}\varsigma\right), & N_\mathrm{r}>N_\mathrm{t}.\end{cases} \tag{46}$$

The upper bounds derived above can be applied to any channel model in the IEEE 802.15.4a standard. For the uncorrelated fading,

- the result in (32) simplifies the integration over the frequency band into the multiplication by the bandwidth in (43), (44), (45) and (46),
- the upper bounds are independent of the AETD, since the uncorrelated fading suppresses the spatial correlation,
- the Jensen upper bound is similar to the trace-plus-Jensen upper bound.

IX. Numerical Examples

The infinite summation in (33) is approximated by $\sum_{L=1}^{\infty}(\cdot)\approx\sum_{L=1}^{M}(\cdot)$, where M is a large number. From the experiment, the approximation is accurate, when M is larger than 10.

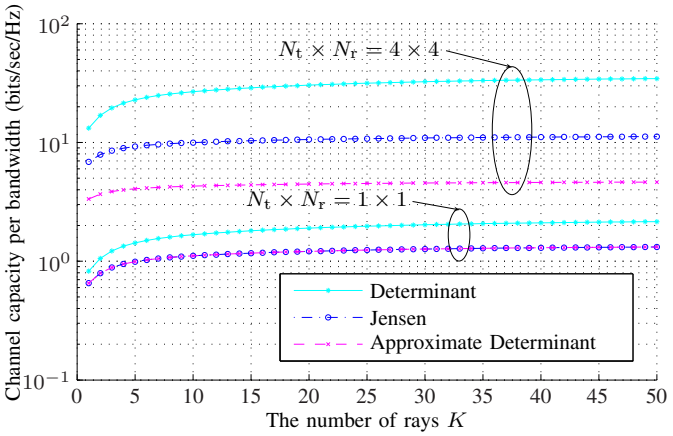

Fig. 1. Channel capacity as a function of the number of the rays K with $M = 50$, $\frac{\sigma_x^2}{\sigma_n^2} = 1$ (SNR = 0 dB) and all relevant parameters according to the CM1 (residential) for LoS scenario [8, Tbl. I].

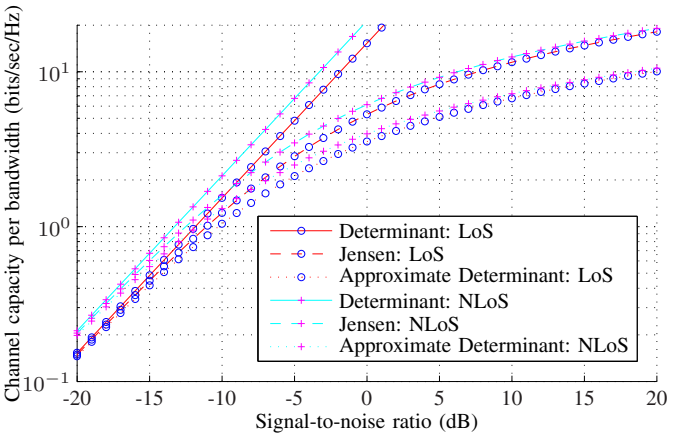

Fig. 2. Channel capacity as a function of the SNR $\frac{\sigma_x^2}{\sigma_n^2}$ with $M = 50$, $K = 100$, $N_r = N_t = 2$ and all relevant parameters according to the CM5 and CM6 for LoS and NLoS scenarios [8, Tbl. III].

In Fig. 1, the channel capacity is shown as a function of the number of the rays K for the multiantenna systems with $N_t = N_r = 1$ and $N_t = N_r = 4$. The transmission rate abruptly increases for approximately the first 10 rays. It can be seen that the channel capacity is limited by a certain number of the rays. It means that the information is conveyed by a number of the rays. This is because the rays that last longer provide a lower signal strength, leading to the irrelevant signal to carry the information. In addition, it is obvious that the multiantenna, $N_t \times N_r = 4 \times 4$, increases the transmission rate.

In Fig. 2, the channel capacity is shown as a function of the transmitted SNR $\frac{\sigma_x^2}{\sigma_n^2}$ for the LoS and NLoS environments in the channel models CM5 (Outdoor LoS) and CM6 (Outdoor NLoS), respectively. It can be seen that the NLoS provides more channel capacity than the LoS. Even though it is derived from the low SNR assumption, the numerical result shows that for a wide range of the SNR the approximate determinant upper bound is lower than the Jensen upper bound.

X. Conclusions and Future Works

We considered the transmission rate over the MIMO-UWB channel based on the IEEE 802.15.4a channel model and the AETD. For the uncorrelated fading, the upper bounds are independent of the AETD. The upper bounds derived above can be applied to several channel models in the IEEE 802.15.4a standard. They serve as a simple computation approach to assess the transmission rate over the UWB communication channels. Numerical examples illustrate that the channel capacity is limited by a certain number of the rays and the NLoS provides a benefit to the channel capacity. In future work, the capacity of the IEEE 802.15.4a multiantenna channel considering the AETD for correlated fading remains a challenging problem.

References

[1] Q. H. Spencer, B. D. Jeffs, M. A. Jensen, and A. L. Swindlehurst, "Modeling the statistical time and angle of arrival characteristics of an indoor multipath channel," *IEEE J. Select. Areas Commun.*, vol. 18, no. 3, pp. 347–360, May 2000.

[2] J. W. Wallace and M. A. Jensen, "Modeling the indoor MIMO wireless channel," *IEEE Trans. Antennas Propagat.*, vol. 50, no. 5, pp. 591–599, May 2002.

[3] X. Hong, C.-X. Wang, J. Thompson, B. Allen, and W. Q. Malik, "Deconstructing space-frequency correlated ultrawideband MIMO channels," in *Proc. IEEE Int. Conf. Ultra-Wideband 2008 (ICUWB 2008)*, vol. 1, Hanover, Germany, Sept. 2008, pp. 47–50.

[4] A. Saleh and R. Valenzuela, "A statistical model for indoor multipath propagation," *IEEE J. Select. Areas Commun.*, vol. 5, no. 2, pp. 128–137, Feb. 1987.

[5] L. H. Brandenburg and A. D. Wyner, "Capacity of the Gaussian channel with memory: The multivariate case," *Bell Syst. Tech. J.*, vol. 53, May-June 1974.

[6] A. F. Molisch, K. Balakrishnan, C.-C. Chong, S. Emami, A. Fort, J. Karedal, J. Kunisch, H. Schantz, U. Schuster, and K. Siwiak, "IEEE 802.15.4a channel model - final report," Institute of Electrical and Electronics Engineers, Inc., Tech. Rep. IEEE 802.15-04-0662-02-004a, Nov. 2004. [Online]. Available: http://grouper.ieee.org/groups/802/15/pub/04/15-04-0662-02-004a-channel-model-final-report-r1.pdf

[7] A. F. Molisch, "Ultrawideband propagation channels-theory, measurement, and modeling," *IEEE Trans. Veh. Technol.*, vol. 54, no. 5, pp. 1528–1545, Sept. 2005.

[8] A. F. Molisch, D. Cassioli, C.-C. Chong, S. Emami, A. Fort, B. Kannan, J. Karedal, J. Kunisch, H. G. Schantz, K. Siwiak, and M. Z. Win, "A comprehensive standardized model for ultrawideband propagation channels," *IEEE Trans. Antennas Propagat.*, vol. 54, no. 11, pp. 3151–3166, Nov. 2006.

[9] M. Nakagami, "The m-distribution—a general formula intensity distribution of rapid fading," in *Statistical Methods in Radio Wave Propagation*, W. C. Hoffman, Ed. New York, NY: Pergamon Press, 1960, pp. 3–35.

[10] H. Hashemi, T.-S. Chu, and J. Roderick, "Integrated true-time-delay-based ultra-wideband array processing," *IEEE Commun. Mag.*, vol. 46, no. 9, pp. 162–172, Sept. 2008.

[11] K. Liu, V. Raghavan, and A. M. Sayeed, "Capacity scaling and spectral efficiency in wide-band correlated MIMO channels," *IEEE Trans. Inform. Theory*, vol. 49, no. 10, pp. 2504–2526, Oct. 2003.

[12] R. A. Horn and C. R. Johnson, *Matrix Analysis*. Cambridge: Cambridge University Press, 1985.

[13] T. M. Cover and J. A. Thomas, *Elements of Information Theory*, 2nd ed. Hoboken, NJ: John Wiley & Sons, 2006.

[14] H. Lütkepohl, *Handbook of Matrices*. West Sussex, England: John Wiley & Sons, 1996.

[15] G. A. F. Seber, *A Matrix Handbook for Statisticians*. Hoboken, NJ: John Wiley & Sons, 2008.

[16] I. S. Gradshteyn and I. M. Ryzhik, *Table of Integrals, Series, and Products*, 7th ed. San Diego, CA: Elsevier, 2007.

[17] W. Gröbner and N. Hofreiter, *Integraltafel: Zweiter Teil—Bestimmte Integrale*. Wien: Springer-Verlag, 1966, Vierte, verbesserte Auflage.

Algebraic Inequalities for MIMO-UWB with Antenna Element Time Delays: Uncorrelated Fading

Bamrung Tau Sieskul, Claus Kupferschmidt, and Thomas Kaiser

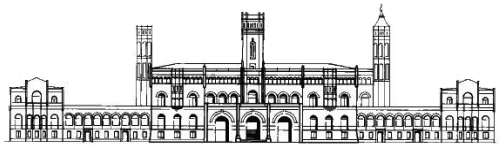

Institute of Communications Technology
Faculty of Electrical Engineering and Computer Science
Leibniz University of Hannover

September 11, 2009

Table of Contents

- Introduction
- Channel Capacity
- IEEE 802.15.4a Channel Model
- MIMO Channel Model
- Inequalities
- Channel Statistics
- Closed Forms of Upper Bounds
- Numerical Examples
- Conclusions and Future Works
- Acknowledgement, Questions, and Comments

Literature Review (I)

- The cluster of the rays is the attribute of the radio propagation [Saleh and Valenzuela 1987][1].
- The extension of Saleh and Valenzuela's cluster model to the directional channel impulse response (see, e.g., [Spencer et al. 2000, eq. (6)][2] at 7 GHz and [Wallace and Jensen 2002, eq. (15)][3] at 2.4 GHz).

[1] [Saleh and Valenzuela 1987] A. Saleh and R. Valenzuela, "A statistical model for indoor multipath propagation," *IEEE J. Select. Areas Commun.*, vol. 5, no. 2, pp. 128-137, Feb. 1987.

[2] [Spencer et al. 2000] Q. H. Spencer, B. D. Jeffs, M. A. Jensen, and A. L. Swindlehurst, "Modeling the statistical time and angle of arrival characteristics of an indoor multipath channel," *IEEE J. Select. Areas Commun.*, vol. 18, no. 3, pp. 347-360, May 2000.

[3] [Wallace and Jensen 2002] J. W. Wallace and M. A. Jensen, "Modeling the indoor MIMO wireless channel," *IEEE Trans. Antennas Propagat.*, vol. 50, no. 5, pp. 591-599, May 2002.

Literature Review (II)

- The propagation across different antenna elements is considered in [Hong et al. 2008][4].
- In [Hong et al. 2008], there is no modeling for the cluster of the rays.

[4] [Hong et al. 2008] X. Hong, C.-X.Wang, J. Thompson, B. Allen, and W. Q. Malik, "Deconstructing space-frequency correlated ultrawideband MIMO channels," in *Proc. IEEE Int. Conf. Ultra-Wideband 2008 (ICUWB 2008)*, vol. 1, Hanover, Germany, Sep. 2008, pp. 47-50.

Transciever Model

- A point-to-point communication transceiver is composed of
  - N_{r} antenna elements at the receiver, and
  - N_{t} antenna elements at the transmitter.
- The received signal $\mathbf{y}(t) \in \mathbb{C}^{N_{\mathrm{r}} \times 1}$ can be expressed as

$$\mathbf{y}(t) = \mathbf{H}(t) * \mathbf{x}(t) + \mathbf{n}(t), \tag{1}$$

where $*$ is the convolution,

- $\mathbf{x}(t) \in \mathbb{C}^{N_{\mathrm{t}} \times 1}$ is the transmitted signal,
- $\mathbf{H}(t) \in \mathbb{C}^{N_{\mathrm{r}} \times N_{\mathrm{t}}}$ is the MIMO channel, and
- $\mathbf{n}(t) \in \mathbb{C}^{N_{\mathrm{r}} \times 1}$ is the additive noise.

Channel Capacity (I)

Theorem (frequency-selective MIMO channel capacity)

Given a frequency-selective channel $\mathbf{H}(t)$ with $\tilde{L}$ multipath components, the channel capacity can be expressed as [Brandenburg and Wyner 1974][5]

$$C = \max_{\mathbf{\Sigma}_{\mathrm{xx}}(f)} \int_{-\frac{1}{2}W}^{\frac{1}{2}W} \log\left(|\mathbf{I}_{(\check{N})} + \mathbf{M}(f)|\right) \mathrm{d}f, \tag{2}$$

where

- $\mathbf{\Sigma}_{\mathrm{xx}}(f)$ *is the power spectral density (PSD) matrix of the transmitted signal, ...*

[5] [Brandenburg and Wyner 1974] L. H. Brandenburg and A. D. Wyner, "Capacity of the Gaussian channel with memory: The multivariate case," *Bell Syst. Tech. J.*, vol. 53, no, 5, May/June 1974.

Channel Capacity (II)

Theorem (frequency-selective MIMO channel capacity (continued))

- W *is the signal bandwidth,*
- $\check{N} = \min(N_\mathrm{t}, N_\mathrm{r})$ *is the minimum number of the transmitter and receiver antennas, and*
- $\mathbf{M}(f) \in \mathbb{C}^{\check{N} \times \check{N}}$ *is the matrix given by*

$$\mathbf{M}(f) = \begin{cases} \mathbf{\Sigma}_{\mathrm{nn}}^{-1}(f)\mathbf{H}_{\tilde{L}}(f)\mathbf{\Sigma}_{\mathrm{xx}}(f)\mathbf{H}_{\tilde{L}}^{\mathrm{H}}(f), & N_\mathrm{r} \leq N_\mathrm{t}, \\ \mathbf{\Sigma}_{\mathrm{xx}}(f)\mathbf{H}_{\tilde{L}}^{\mathrm{H}}(f)\mathbf{\Sigma}_{\mathrm{nn}}^{-1}(f)\mathbf{H}_{\tilde{L}}(f), & N_\mathrm{r} > N_\mathrm{t}, \end{cases} \tag{3}$$

with

- $\mathbf{H}_{\tilde{L}}(f)$ *being the Fourier transform of the channel, and*
- $\mathbf{\Sigma}_{\mathrm{nn}}(f)$ *being the PSD of the stationary Gaussian noise.*

Ergodic Channel Capacity

- Assume that there exist $\tilde{N}$ random parameters, which are collected in $\boldsymbol{\eta} \in \mathbb{R}^{\tilde{N} \times 1}$, residing in $\mathbf{M}(f)$.
- When each element of $\boldsymbol{\eta}$ is an ergodic process, the ergodic capacity is written as

$$\bar{C} = \frac{1}{\ln(2)} \int_{-\frac{1}{2}W}^{\frac{1}{2}W} \mathrm{E}_{\boldsymbol{\eta}} \left\{ \max_{\boldsymbol{\Sigma}_{\mathrm{xx}}(f)} \ln\left(|\mathbf{I} + \mathbf{M}(\boldsymbol{\eta}, f)|\right) \right\} \mathrm{d}f. \qquad (4)$$

IEEE 802.15.4a Channel Model (I)

The impulse response of the IEEE 802.15.4a channel can be expressed as (see, e.g., [Molisch et al. 2004][6], [Molisch 2005][7], and [Molisch et al. 2006][8])

$$h(t) = \sum_{l=0}^{L} \sum_{k=0}^{K} a[k,l] \mathrm{e}^{\mathrm{j}\upsilon[k,l]} \delta(t - T[l] - \tau[k,l]), \qquad (5)$$

[6] [Molisch et al. 2004] A. F. Molisch, K. Balakrishnan, C.-C. Chong, S. Emami, A. Fort, J. Karedal, J. Kunisch, H. Schantz, U. Schuster, and K. Siwiak, "IEEE 802.15.4a channel model - final report," Institute of Electrical and Electronics Engineers, Inc., Tech. Rep. IEEE 802.15-04-0662-02-004a, Nov. 2004. [Online]. Available: http://grouper.ieee.org/groups/802/15/pub/04/15-04-0662-02-004a-channel-model-final-report-r1.pdf

[7] [Molisch 2005] A. F. Molisch, "Ultrawideband propagation channels-theory, measurement, and modeling," *IEEE Trans. Veh. Technol.*, vol. 54, no. 5, pp. 1528-1545, Sept. 2005.

[8] [Molisch et al. 2006] A. F. Molisch, D. Cassioli, C.-C. Chong, S. Emami, A. Fort, B. Kannan, J. Karedal, J. Kunisch, H. G. Schantz, K. Siwiak, and M. Z. Win, "A comprehensive standardized model for ultrawideband propagation channels," *IEEE Trans. Antennas Propagat.*, vol. 54, no. 11, pp. 3151-3166, Nov. 2006.

IEEE 802.15.4a Channel Model (II)

where

- $L+1$ is the number of clusters, $K+1$ is the number of multipath rays assumed to be equal in each cluster,
- $a[k,l]$ is the tap weight of the k-th component in the l-th cluster,
- $\upsilon[k,l]$ is the corresponding phase shift, and
- $\tau[k,l]$ is the delay of the k-th multipath component relative to the l-th cluster arrival time $T[l]$.

Antenna Element Propagation Delay

- For the k-th cluster and the l-th path,
  - the angle of departure induces the propagation delay $\frac{1}{c}(n_{\mathrm{t}}-1)d\sin(\theta[k,l])$ at the n_{t}-th transmitter antenna, and
  - the angle of arrival induces the propagation delay $\frac{1}{c}(n_{\mathrm{r}}-1)d\sin(\phi[k,l])$ at the n_{r}-th receiver antenna.
- To capture the time delay across antenna elements at both sides, the impulse response can be written as

$$h^{k,l}_{n_{\mathrm{r}},n_{\mathrm{t}}}(t) = \delta(t-\psi_{n_{\mathrm{r}},n_{\mathrm{t}}}[k,l]), \tag{6}$$

where

- the propagation delay $\psi_{n_{\mathrm{r}},n_{\mathrm{t}}}[k,l]$ is given by

$$\psi_{n_{\mathrm{r}},n_{\mathrm{t}}}[k,l] = \frac{1}{c}d\left((n_{\mathrm{t}}-1)\sin(\theta[k,l]) + (n_{\mathrm{r}}-1)\sin(\phi[k,l])\right). \tag{7}$$

Effective Channel Model

The effective channel impulse response can be shown as

$$\begin{aligned} h_{n_\mathrm{r},n_\mathrm{t}}(t) &= h(t) * h^{k,l}_{n_\mathrm{r},n_\mathrm{t}}(t) \\ &= \sum_{l=0}^{L}\sum_{k=0}^{K} \alpha_{n_\mathrm{r},n_\mathrm{t}}[k,l]\delta(t - T[l] - \tau[k,l] - \psi_{n_\mathrm{r},n_\mathrm{t}}[k,l]), \end{aligned} \tag{8}$$

where

- $\alpha_{n_\mathrm{r},n_\mathrm{t}}[k,l]$ is the antenna-dependent complex amplitude given by

$$\alpha_{n_\mathrm{r},n_\mathrm{t}}[k,l] = a_{n_\mathrm{r},n_\mathrm{t}}[k,l]\mathrm{e}^{\mathrm{j}\upsilon_{n_\mathrm{r},n_\mathrm{t}}[k,l]}. \tag{9}$$

Jensen Upper Bound

The ergodic capacity can be upper bounded by

$$\bar{C} \leq \bar{B}_{\text{Jensen}} = \frac{1}{\ln(2)} \int_{-\frac{1}{2}W}^{\frac{1}{2}W} \ln\left(\left|\mathbf{I} + \mathrm{E}_{\boldsymbol{\eta}}\left\{\mathbf{M}(\boldsymbol{\eta}, f)\right\}\right|\right) \mathrm{d}f, \qquad (10)$$

where the inequality is derived from the Jensen's inequality of the real-valued concave function[9] $\ln(|\cdot|)$.

[9] Concavity of a continuous function $f(\cdot)$ satisfies $\frac{1}{2}\left(f(x) + f(y)\right) \leq f\left(\frac{1}{2}(x+y)\right)$.

Determinant Upper Bounds (I)

- An inequality of the determinant reads as (see, e.g., [Lütkepohl 1996, p. 55][10])

$$\ln(|\mathbf{M}|) \leq \mathrm{tr}(\mathbf{M}) - \check{N}. \tag{11}$$

- We can write

$$\bar{C} \leq \bar{B}_{\mathrm{det}} = \frac{1}{\ln(2)} \int_{-\frac{1}{2}W}^{\frac{1}{2}W} \mathrm{tr}\left(\mathrm{E}_{\boldsymbol{\eta}}\left\{\mathbf{M}(\boldsymbol{\eta}, f)\right\}\right) \mathrm{d}f. \tag{12}$$

[10] [Lütkepohl 1996] H. Lütkepohl, *Handbook of Matrices*. West Sussex, England: John Wiley & Sons, 1996.

Determinant Upper Bounds (II)

- We can expand (see, e.g., [Seber 2008, p. 312][11])

$$|\mathbf{I}+\frac{\sigma_{\mathrm{x}}^2}{\sigma_{\mathrm{n}}^2}\breve{\mathbf{M}}(\boldsymbol{\eta},f)| = 1+\frac{\sigma_{\mathrm{x}}^2}{\sigma_{\mathrm{n}}^2}\mathrm{tr}\left(\breve{\mathbf{M}}(\boldsymbol{\eta},f)\right)+O\left(\left(\frac{\sigma_{\mathrm{x}}^2}{\sigma_{\mathrm{n}}^2}\right)^2\right). \quad (13)$$

- The ergodic capacity can be approximated by

$$\begin{aligned}\bar{C} \simeq \tilde{C} &= \frac{1}{\ln(2)}\int_{-\frac{1}{2}W}^{\frac{1}{2}W} \mathrm{E}_{\boldsymbol{\eta}}\left\{\ln\left(1+\mathrm{tr}\left(\mathbf{M}(\boldsymbol{\eta},f)\right)\right)\right\}\mathrm{d}f \\ &\leq \tilde{C}_{\mathrm{approdet}} = \frac{1}{\ln(2)}\int_{-\frac{1}{2}W}^{\frac{1}{2}W} \ln\left(1+\mathrm{E}_{\boldsymbol{\eta}}\left\{\mathrm{tr}\left(\mathbf{M}(\boldsymbol{\eta},f)\right)\right\}\right)\mathrm{d}f, \end{aligned} \quad (14)$$

where the inequality holds from the concavity of $\ln(\cdot)$.

[11] [Seber 2008] G. A. F. Seber, *A Matrix Handbook for Statisticians*. Hoboken, NJ: John Wiley & Sons, 2008.

Trace Upper Bounds

Using $\ln(|\mathbf{M}|) \leq \check{N}\left(\ln\left(\mathrm{tr}(\mathbf{M})\right) - \ln(\check{N})\right)$ (see, e.g., [Lütkepohl 1996, p. 43]), the capacity is upper bounded by

$$\begin{aligned}\bar{C} &\leq \bar{B}_{\mathrm{tr}} = \frac{\check{N}}{\ln(2)} \int_{-\frac{1}{2}W}^{\frac{1}{2}W} \mathrm{E}_{\boldsymbol{\eta}} \left\{ \ln\left(1 + \frac{1}{\check{N}} \mathrm{tr}\left(\mathbf{M}(\boldsymbol{\eta}, f)\right)\right)\right\} \mathrm{d}f \\ &\leq \bar{B}_{\mathrm{tr+Jensen}} = \frac{\check{N}}{\ln(2)} \int_{-\frac{1}{2}W}^{\frac{1}{2}W} \ln\left(1 + \frac{1}{\check{N}} \mathrm{E}_{\boldsymbol{\eta}} \left\{\mathrm{tr}\left(\mathbf{M}(\boldsymbol{\eta}, f)\right)\right\}\right) \mathrm{d}f, \end{aligned} \tag{15}$$

where the last inequality holds from the Jensen inequality according to the concavity of $\ln(\cdot)$.

Amplitude Correlation

- From the power delay profiles (PDPs) of the line of sight and non-line of sight, there is no correlation for the contributions between k and $\acute{k}$ as well as between l and $\acute{l}$.
- Then, we have

$$\begin{aligned}\mathbf{\Sigma_{AA}}[k,l,\acute{k},\acute{l}] &= \mathrm{E}\left\{\mathrm{vec}(\tilde{\mathbf{A}}[k,l])\mathrm{vec}^{\mathrm{T}}(\tilde{\mathbf{A}}[\acute{k},\acute{l}])\right\} \\ &= \delta_{k,\acute{k}}\delta_{l,\acute{l}}\mathrm{E}\left\{|a[k,l]|^2|\tau[k,l]\right\}\mathbf{I}_{(N_{\mathrm{r}}N_{\mathrm{t}})},\end{aligned} \tag{16}$$

where $\mathrm{E}\left\{|a[k,l]|^2|\tau[k,l]\right\}$ is the PDP depending on each channel model.

Closed Forms of the Upper Bounds

We have the following closed forms of the upper bounds

$$\bar{B}_{\text{Jensen}} = \begin{cases} \frac{1}{\ln(2)} W N_{\text{r}} \ln\left(1 + \frac{\sigma_{\text{x}}^2}{\sigma_{\text{n}}^2} N_{\text{t}} \varsigma\right), & N_{\text{r}} \leq N_{\text{t}}, \\ \frac{1}{\ln(2)} W N_{\text{t}} \ln\left(1 + \frac{\sigma_{\text{x}}^2}{\sigma_{\text{n}}^2} N_{\text{r}} \varsigma\right), & N_{\text{r}} > N_{\text{t}}, \end{cases} \tag{17}$$

$$\bar{B}_{\text{det}} = \frac{1}{\ln(2)} \frac{\sigma_{\text{x}}^2}{\sigma_{\text{n}}^2} W N_{\text{r}} N_{\text{t}} \varsigma, \tag{18}$$

$$\tilde{C}_{\text{approdet}} = \frac{1}{\ln(2)} W \ln\left(1 + \frac{\sigma_{\text{x}}^2}{\sigma_{\text{n}}^2} N_{\text{r}} N_{\text{t}} \varsigma\right), \tag{19}$$

where ς is given by

$$\varsigma = \sum_{L=1}^{\infty} \frac{1}{L!} \bar{L}^L \mathrm{e}^{-\bar{L}} \sum_{l=0}^{L} \sum_{k=0}^{K} \mathrm{E}_{\tau,T,M_{\text{c}}} \left\{ |a[k,l]|^2 | \tau[k,l] \right\}. \tag{20}$$

The Number of Sums

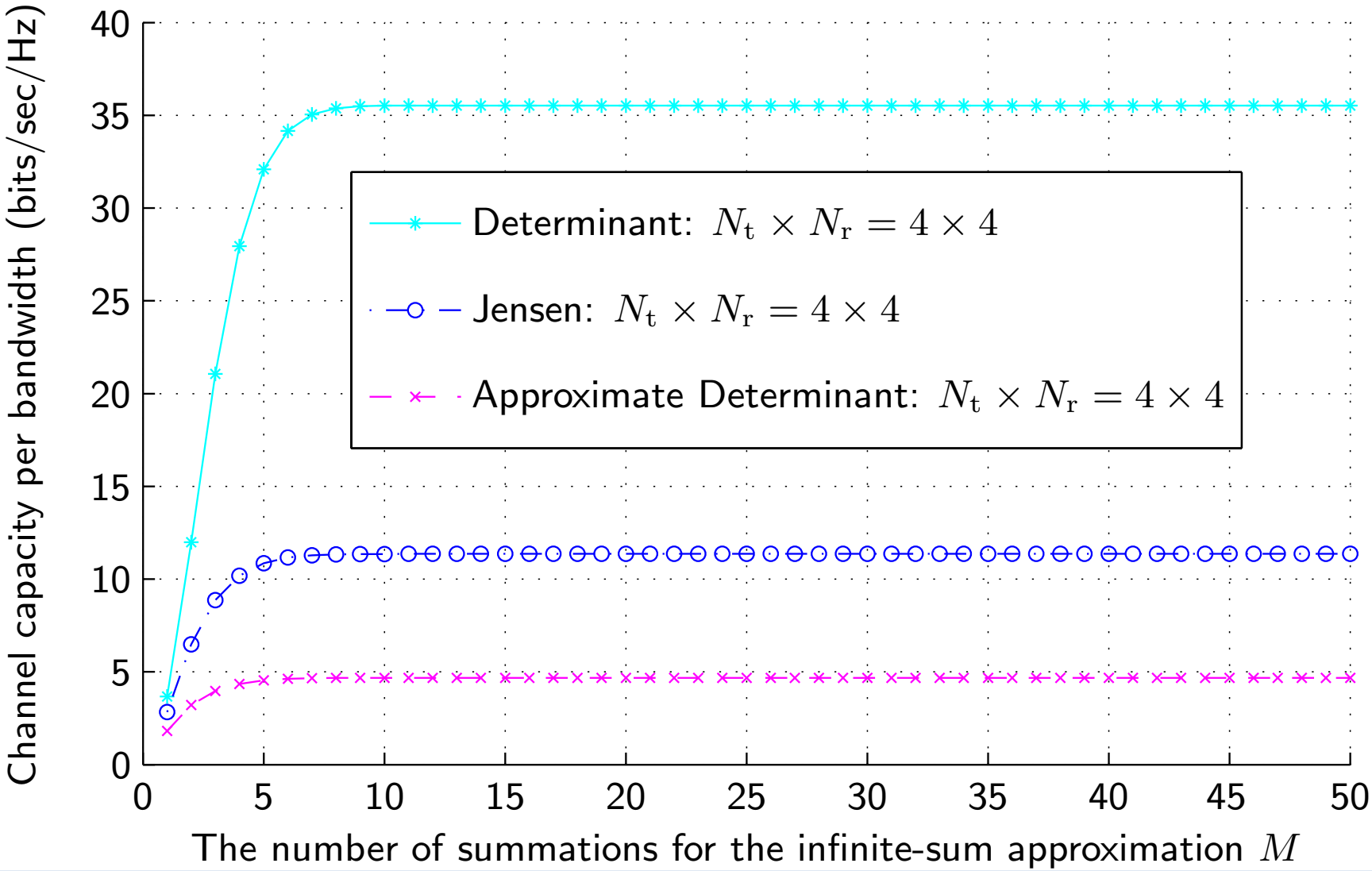

The Number of Rays

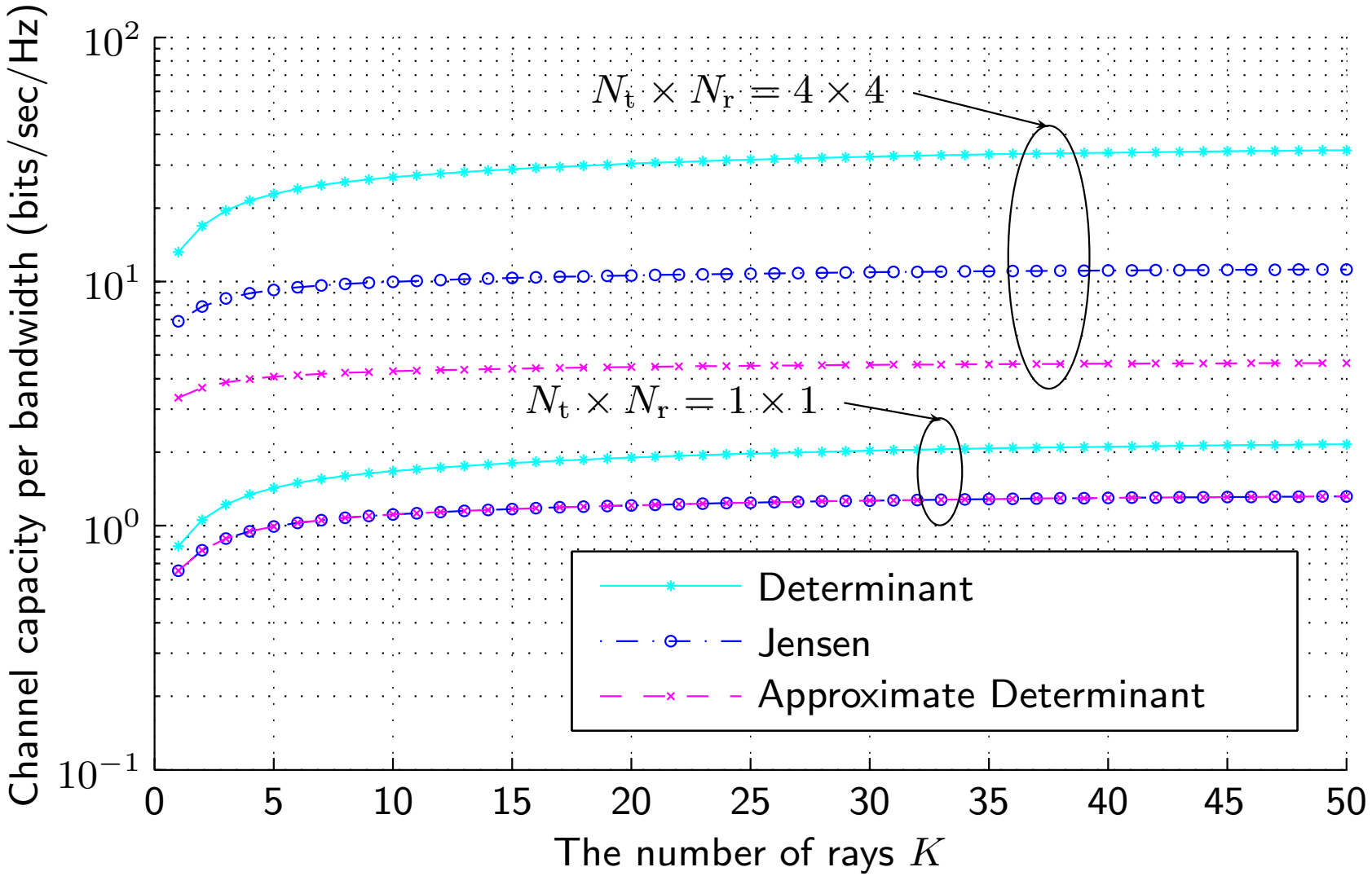

Signal-to-Noise Ratio

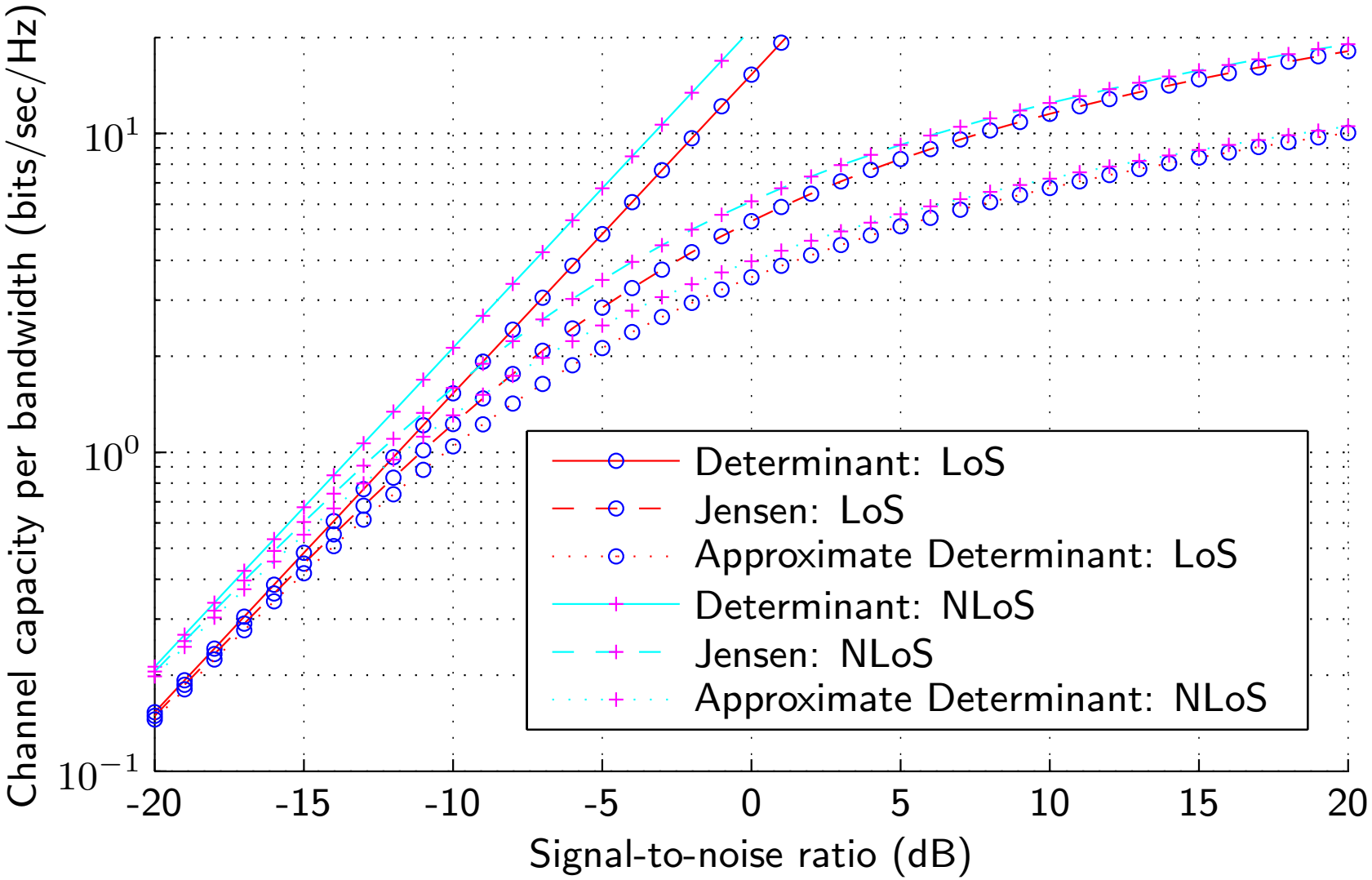

Conclusions and Future Works

- We considered the transmission rate over the MIMO-UWB channel based on the IEEE 802.15.4a channel model and the AETD.
- For the uncorrelated fading, the upper bounds are independent of the AETD.
- The channel capacity is limited by a certain number of the rays.
- The NLoS provides a benefit to the channel capacity.
- Correlated fading remains a challenging problem.

Acknowledgement, Questions, and Comments

An integrated European R&D Project - coExisting short range radio by advanced Ultra-WideBand radio technology (EUWB).

Thank you for your attention.